

25 **Abstract**

26 The use of phononic crystals and elastic metamaterials has been a significant
27 concern as an efficient approach to attenuate the surface waves of ambient vibration
28 and seismic vibration. In previous research, elastic metamaterials with periodic array
29 of pillars or other forms of standing structures (such as H-fractal steel or built-up
30 structural steel) erected on soil substrate can achieve a low frequency surface wave
31 band gap (BG). However, such metamaterials with standing structures occupy land and
32 affect the esthetics of cities, and buried metamaterials such as cross-like-cavity or
33 hollow-cylinder structures with large size in soils necessitate continual maintenance for
34 the stability of cavity soil structure. Thus, this study proposes two types of periodic
35 hollow steel trenches exhibiting both a Bragg BG and a local resonance BG, the steel
36 plates are used to support the soil on both sides of the trench to meet the stability
37 requirements of cavity soil structure and avoid toppling or landslide of soils. The
38 dispersion relations of periodic hollow steel trenches are calculated by using finite
39 element method and the mechanism of generation for two kinds of BGs are interpreted
40 by the eigenmodes. Furthermore, the effectiveness of periodic hollow steel trenches on
41 isolating surface waves within the BGs is demonstrated in both frequency domain and
42 time domain analysis. Several significant geometrical and material parameters on BGs
43 that can affect the BG are studied as well. This study provides a new approach using
44 the coupling effects of Bragg BG and local resonance BG to simultaneously attenuate
45 the surface waves induced by the ambient and seismic vibration in a more practical way.

46 **Keywords:** surface waves; periodic structure; band gap; Bragg scattering; local

47 resonance.

48 **1. Introduction**

49 Excessive vibrations caused by traffic, construction activity, machine operation and
50 earthquake cause damage to adjacent structures and residents, such as disturbing
51 residents health, affecting the work of delicate instruments, even destroying buildings
52 and threatening human lives [1]. Surface waves (Rayleigh waves) at middle and low
53 frequencies have received more research attention due to the fact that they can travel
54 further, decay slowly along the ground and be potentially more disruptive. Therefore,
55 the methods of ground vibration attenuation by constructing wave barriers such as open
56 trenches, infilled trenches, pile barriers, etc across the propagation paths of surface
57 waves in soils has received more research attention and become a major concern in
58 recent years [2-10]. These wave barriers in half-space soils may intercept, scatter or
59 diffract incident surface waves sufficiently to reduces their amplitudes. The open trench
60 is the most effective measure to isolate surface waves among any other wave barrier,
61 because its stress-free boundaries act as perfect reflectors of waves [6-10]. However,
62 its practical application is limited to relatively shallow depths due to the instability of
63 soils and water table, and it may be turned to a water-filled trench caused by the
64 fluctuation of water table, which can result in the efficiency reduction of vibration
65 isolation and environmental problems such as mosquito breeding and germ spreading
66 due to the contamination of water [10]. In addition, the open trench in public places
67 may pose a serious threat to security of pedestrian. By contrast, the proposed hollow
68 steel trench exhibits practical values in engineering. On the one hand, the form of

69 hollow steel trench (like a cavity structure) is similar to that of open trench, which
70 means it can provide a desirable vibration reduction effectiveness. On the other hand,
71 the use of hollow steel trench can necessitate no continual maintenance of trench
72 structure and no treat to health and security of residents, because the steel plates can
73 support the soil on both sides of the trench to meet the requirements of soil stability and
74 avoid toppling or landslide.

75 Recently, the research of phononic crystals [11-13] and elastic metamaterials [14-
76 16] has promoted the study of periodic wave barriers for vibration mitigation based on
77 the band gap (BG), frequency regions where waves are prohibited from propagation. It
78 is well-known that most of energy of ambient or seismic vibration is carried by surface
79 waves and they travel further, decay more slowly along the ground than body waves.
80 BGs can be achieved to cover the frequencies domain of ambient or seismic vibration
81 with a rational design of periodic trenches [17-20], periodic pile barriers [21-24] and
82 seismic metamaterials [25-30]. Mechanisms for the BG generation are classified as
83 Bragg scattering and local resonance. Bragg scattering originates from the spatial
84 periodicity of the impedance mismatch and results from the destructive interference of
85 incident and scattered waves, occurring at wavelengths being comparable to unit cell
86 sizes [11-13]. Distinct from the Bragg scattering mechanism, the relevant wavelength
87 with regard to the local resonance is much larger than unit cell sizes, which contributes
88 to opening the BG at low frequencies. Local resonance mechanism stems from the
89 hybridization effect between the bands of the resonant modes inside the units and the
90 propagating modes of the substrate media [14].

91 Surface wave BGs around middle frequencies were obtained based on Bragg
92 scattering in the research of the periodic trench barriers, which can be available for the
93 application in the ambient vibration isolation [17-20]. Periodic geof foam-filled trenches
94 [17,18], periodic composite infilled trenches [19] and layered periodic structures [20]
95 were verified as effective wave barriers to attenuate surface waves induced by trains,
96 and these surface wave BGs were obtained from 40 Hz to 70 Hz. Different from the
97 Bragg BG, the local resonance BG appearing in the periodic pile barriers and elastic
98 metamaterials was around low frequencies (below 20 Hz), which can be used to
99 safeguard large infrastructures from seismic threats [21-31]. Additionally, a pillared
100 metamaterial in phononics which was composed of periodic arrangement of pillars
101 erected on a plate provides a new tool to manipulate the propagation of surface waves.
102 It is interesting that Bragg BG and local resonance BG can be simultaneously observed
103 in pillared metamaterials [32-35], the Bragg BG is induced by the system's periodicity
104 and local resonance BG is originated from the occurrence of branching pillars acting as
105 the local resonators. It is possible for using such metamaterials to simultaneously
106 attenuate the surface waves in ambient vibration at middle frequencies and shield the
107 seismic waves at low frequencies. Some researchers further proposed the hollow pillar
108 metamaterials, localized modes relative to low-frequency BG were synthesized by
109 introducing hollow parts in the pillars. As the existence of whispering-gallery modes
110 (WGMs), the local resonance BG was shifted toward extremely low frequencies and
111 the Bragg BG became much wider [36,37].

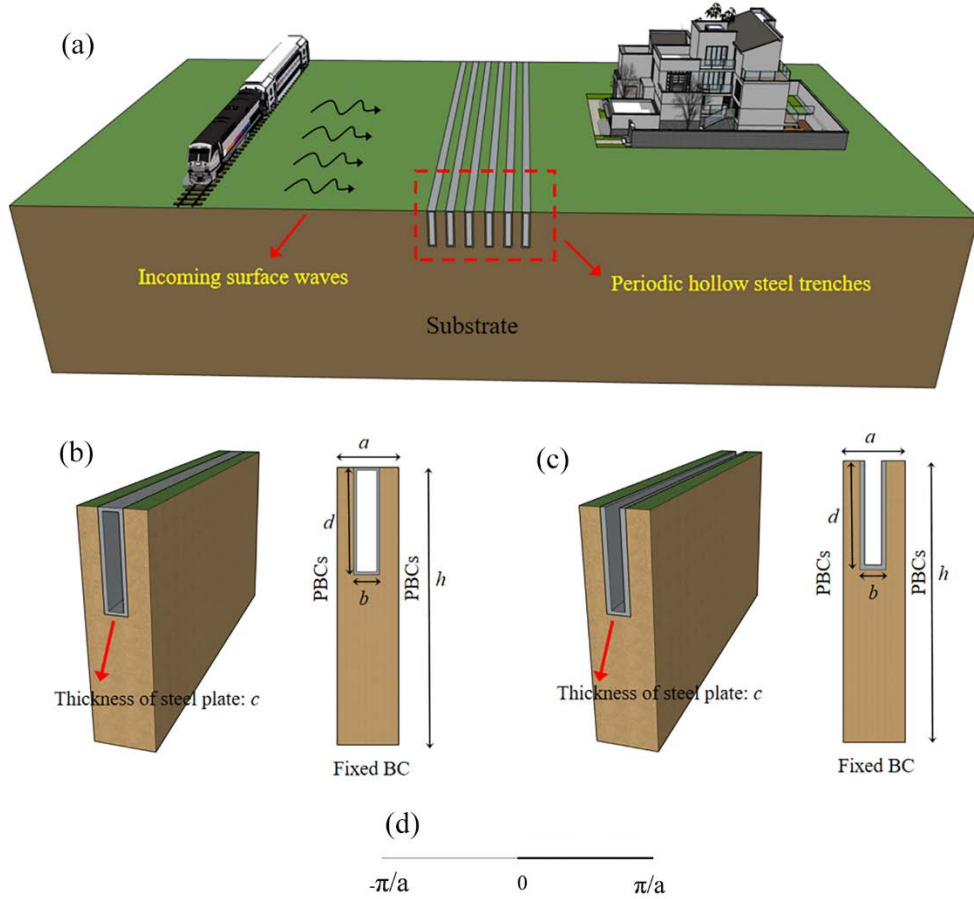
112 However, elastic metamaterials consisted of a periodic arrangement of hollow

113 pillars or other forms of standing structures such as H-fractal steel [25] or built-up
114 structural steel [26] standing on the ground, which can occupy land and affect the
115 esthetics of cities. Lots of elastic metamaterials were buried in a semi-infinite soil for
116 the control and manipulation of surface waves propagation [28,29,31,38], but it was not
117 easy to maintain the stability of the cavity soil structure such as cross-like-cavity or
118 hollow-cylinder structures with large size in soils [31]. In this study, two types of
119 periodic hollow steel trenches featuring both Bragg BG and local resonance BG are
120 proposed. Steel plates are exploited to maintain the stability of soils on both sides of
121 the trench and avoid the toppling or landslide, which can be conducive to practical
122 engineering applications. We also explore the generation mechanism of Bragg BG and
123 local resonance BG appearing in periodic hollow steel trenches. Furthermore, the
124 desired performance of vibration mitigation for periodic hollow steel trenches within
125 Bragg BG and local resonance BG are validated in frequency domain and time domain
126 analysis. Finally, parametric analyses are carried out to analyze the effect of
127 geometrical and material parameters on BGs. The aim of this study is to achieve Bragg
128 BG and local resonance BG in both middle frequencies and low frequencies
129 respectively with periodic hollow steel trenches, which open up new perspectives for
130 the isolation of ambient or seismic vibration in the field of civil engineering.

131 **2. Methodology and modeling**

132 [Fig. 1\(a\)](#) shows the surface wave attenuation by embedding periodic trenches in a
133 semi-infinite substrate (brown). In this paper, two types of trenches are considered
134 namely periodic hollow sealed steel trenches and periodic hollow unsealed steel

135 trenches respectively, and the Fig. 1 (b) and (c) present the typical unit cells with
136 periodic boundary conditions (PBCs) in respect of two types of periodic trenches. The
137 hollow sealed steel trench in Fig. 1(b) is achieved by filling open trench with a hollow
138 sealed steel frame (dark grey), and the hollow unsealed steel trench in Fig. 1(c) is
139 obtained by filling open trench with a hollow unsealed steel frame (dark grey). A hollow
140 steel trench which is a cavity structure similar to the open trench can provide a desirable
141 vibration isolation effectiveness, and rely on steel plates to support the soil on both
142 sides of the open trench to meet the requirements of soil stability. Moreover, hollow
143 steel trenches are embedding periodic trenches in a semi-infinite substrate, which can
144 block the surface waves falling into the BGs effectively. In addition, there are new local
145 resonance band gaps by using periodic hollow steel trenches compared with using
146 periodic in-filled trenches, which will be discussed in the following analysis. As can be
147 seen from the Fig. 1(b) and (c), a is the lattice constant of two types of trenches, b is the
148 width of trenches, d is the depth of trenches, c is the thickness of steel plate and h is the
149 depth of the soil. Corresponding material properties and geometrical parameters of
150 periodic hollow steel trenches are summarized in Tables 1 and 2, respectively.



151

152 Fig. 1 (a) A schematic diagram of the periodic trenches; (b) unit cell of periodic hollow
 153 sealed steel trench; (c) unit cell of hollow unsealed steel trench; (d) the corresponding
 154 first irreducible Brillouin zone.

155

Table 1. Material parameters

Material	Young's modulus E (MPa)	Poisson ration ν	Density ρ (kg/m ³)
Soil [5,17]	46	0.25	1800
steel	210,000	0.22	7856

156

Table 2. Geometrical parameters

a (m)	b (m)	d (m)	c (m)	h (m)
0.75	0.2	2	0.02	15

157

158 Assuming a homogeneous linear elastic medium with no damping, the governing
 159 equation can be written as:

160

$$\nabla \cdot (\mathbf{C}(\mathbf{r}) : \nabla \mathbf{u}(\mathbf{r})) = \rho(\mathbf{r}) \frac{\partial^2 \mathbf{u}(\mathbf{r})}{\partial t^2}, \quad (1)$$

162 where ∇ represents the differential operator, $\mathbf{r} = (x, y, z)$ represents the position vector,163 $\mathbf{C}(\mathbf{r})$, $\mathbf{u}(\mathbf{r})$ and $\rho(\mathbf{r})$ represent the position-dependent elastic tensor, displacement vector164 and mass density, respectively. t is the time parameter. As per the Bloch-Floquet

165 theorem of solid-state physics, the displacement vector can be expressed as:

$$\mathbf{u}(\mathbf{r}, t) = e^{i(\mathbf{k} \cdot \mathbf{r} - \omega t)} \mathbf{u}_{\mathbf{k}}(\mathbf{r}), \quad (2)$$

167 where ω is the circular frequency, \mathbf{k} is the Bloch-Floquet wave vector limited in the168 first Brillouin zone, and $\mathbf{u}_{\mathbf{k}}(\mathbf{r})$ is a modulation function of the displacement vector. For169 the periodic trenches, $\mathbf{u}_{\mathbf{k}}(\mathbf{r})$ is a periodic function defined in a unit cell, which can be

170 written as:

$$\mathbf{u}_{\mathbf{k}}(\mathbf{r} + \mathbf{a}) = \mathbf{u}_{\mathbf{k}}(\mathbf{r}), \quad (3)$$

172 where \mathbf{a} is the periodic constant vector for periodic structure. Substituting Eq. (3) into

173 Eq. (2), the PBC of a unit cell is acquired as:

$$\mathbf{u}_{\mathbf{k}}(\mathbf{r} + \mathbf{a}, t) = e^{i\mathbf{k} \cdot \mathbf{a}} \mathbf{u}_{\mathbf{k}}(\mathbf{r}, t). \quad (4)$$

175 By combining the displacement vector of Eq. (1) and the periodic boundary

176 condition of Eq. (4), the dispersion analysis of the periodic trenches can be transferred

177 into the solution of eigenfrequency equation:

$$(\tilde{\mathbf{K}} - \omega^2 \tilde{\mathbf{M}}) \cdot \mathbf{u} = 0, \quad (5)$$

179 where $\tilde{\mathbf{K}}$ and $\tilde{\mathbf{M}}$ are the stiffness and mass matrices of a unit cell, respectively. The180 stiffness matrix $\tilde{\mathbf{K}}$ represents a function of the Bloch-Floquet wave vector \mathbf{k} . The181 eigenfrequency ω and the dispersion relationship of the periodic trenches are achieved182 by scanning the wave vector \mathbf{k} in the first irreducible Brillouin zone as shown in Fig.

183 1(d). In this study, the finite element method simulation using software (COMSOL
184 Multiphysics 5.6) is performed to solve the eigenvalue equation and dispersion relations.

185 **3. Results and discussions**

186 *3.1 Dispersion curves for different periodic trenches and Vibration modes*

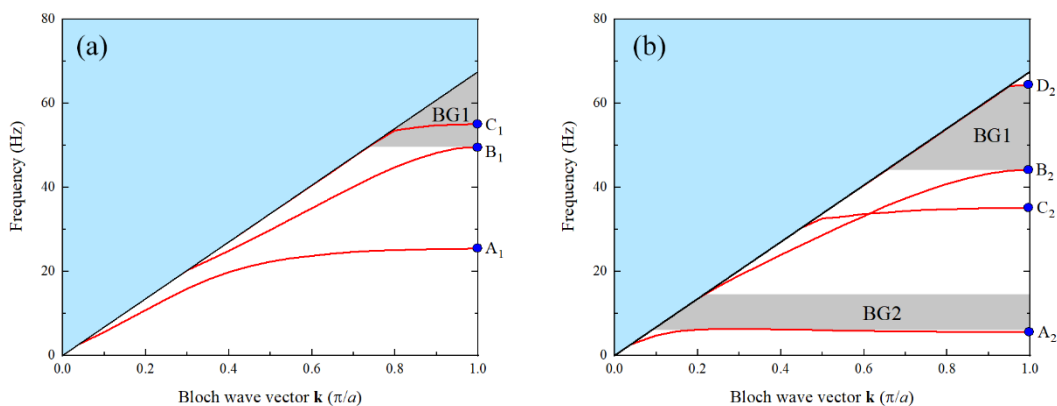
187 The unit cell models in respect of two types of hollow steel trenches are show in
188 Fig. 1 (a) and (b), geometrical parameters and material properties can be seen from
189 Table 1 and 2. A free triangular mesh is used to discretize the models. The maximum
190 element size is 0.225 m, which is smaller than 1/5 of the minimum Rayleigh wavelength
191 at 80 Hz and can contribute to the accurate simulation of waves with frequencies below
192 the 80 Hz. The dispersion relations of periodic two types of trenches are illustrated in
193 Fig. 2, where the thick black solid line is sound line and the shaded areas represent the
194 band gaps. The sound cone method is adopted to obtain surface modes in dispersion
195 relations [39]. The sound line is governed by the formula $w = \mathbf{k} \cdot \mathbf{v}_s$, where $v_s = \sqrt{E/\rho}$
196 is the shear wave velocity of the soil substrate, E and ρ are the shear modulus and
197 density of the soil substrate respectively. The surface modes are located inside the
198 sound cone, while the bulk modes are outside it [40]. The existence of a BG is indicated
199 by the absence of eigenvalues in some frequency ranges.

200 With respect to periodic hollow sealed steel trenches, BG1 is 49.7-67.6 Hz as
201 presented in Fig. 2 (a). The vibration eigenmode at the point B₁ is a kind of guided
202 surface wave modes as shown in Table 3, and such guided surface states correspond to
203 typical Rayleigh-wave modes because of sin-like or cos-like displacement fields, which
204 capture the localization of wave motion near the free surface [18]. Therefore, the band

205 with point B_1 below the sound cone in the Fig. 2 (a) is called surface wave band, the
206 lower boundary of BG1 is dependent on the surface wave modes B_1 , and it can be
207 deduced that BG1 is caused by the system's periodicity, so BG1 is called Bragg BG. It
208 is also interesting that there are two new resonant bands, one appears below the surface
209 wave band and another appears in the Bragg BG around in 55 Hz. Table 3 illustrates
210 the vibration eigenmode at the point A_1 , B_1 , C_1 . Note that the vibration modes at point
211 A_1 and C_1 are locally resonant modes, and the main energy mainly occurs on the both
212 sides of trench.

213 As regards periodic hollow unsealed steel trenches, a new surface wave band
214 appears below the sound cone and a wider Bragg BG (BG1) is 44.2-64.4 Hz as shown
215 in Fig. 2 (b). Compared with periodic hollow sealed steel trenches, two resonance bands
216 are shifted to low frequency and a new narrow band gap appears in a low frequency
217 range from 6.3 to 14.1 Hz, where this new BG (BG2) is called locally resonant BG. The
218 type of band gap in the dispersion curve can be determined by the vibration modes of
219 the upper and lower boundaries of the BG. It can be observed from Table 4 that the
220 vibration eigenmode at the point B_2 , D_2 are the surface wave mode where elastic energy
221 confined near the free surface, besides the vibration modes at point A_2 and C_2 are locally
222 resonant mode where vibration energy is concentrated in the steel plates and soil on
223 both sides of the trench. The upper and lower boundaries of BG1 are dependent on the
224 surface wave modes B_2 and D_2 , and it can be concluded that BG1 is caused by the
225 artificial periodic condition, so BG1 is a Bragg BG. On the other hand, the locally
226 resonant mode A_2 determine the lower boundary of BG2, so BG2 is referred to as

227 locally resonant BG. When resonance is reached, the wave energy is confined inside
 228 the steel plates and soil on both sides of the trench and the energy transmission through
 229 the trench array is strongly reduced. Compared with periodic hollow sealed steel
 230 trenches, the Bragg BG of periodic hollow unsealed steel trenches moves towards low
 231 frequency and a new locally resonant BG appears in low frequency caused by a
 232 downward shift of the fourth band. It is because that there is no top steel plate to limit
 233 the axial displacement of lateral soils and steel plates in the hollow unsealed steel
 234 trenches, such structures with large flexibility can provide larger displacement space
 235 for local resonance.



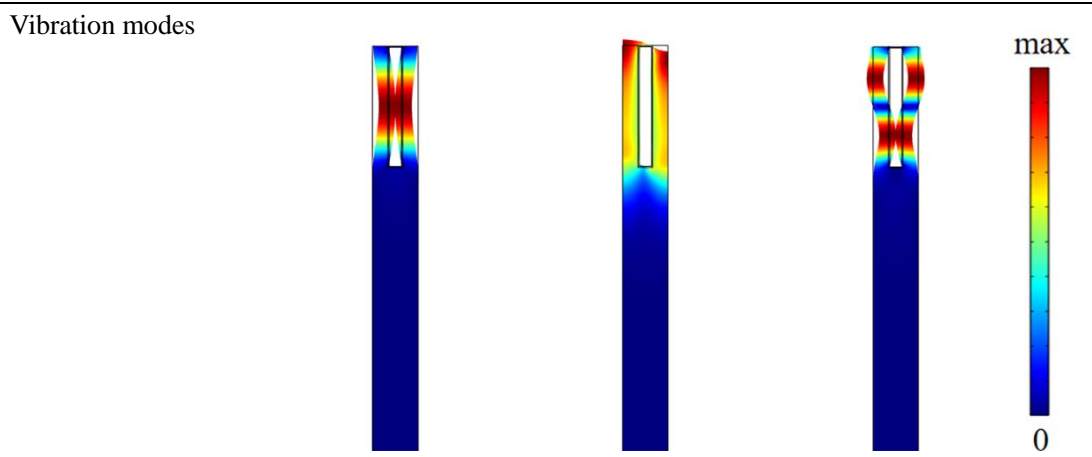
236
 237

238 Fig. 2 Dispersion curves of (a) periodic hollow sealed steel trenches, (b) periodic hollow
 239 unsealed steel trenches.

240

241 Table 3. Vibration modes of periodic hollow sealed steel trenches

Order of vibration	A ₁	B ₁	C ₁
Frequency (Hz)	25.4	49.7	55.1



242

243 Table 4. Vibration modes of periodic hollow unsealed steel trenches

Order of vibration	A ₂	B ₂	C ₂	D ₂
Frequency (Hz)	5.6	44.2	35.2	64.4
Vibration modes				

244

245 3.2 Frequency domain analysis

246 The BGs of two types of periodic hollow steel trenches are analyzed on basis of the
 247 infinite unit cell mode, whereas the periodic wave barriers are finite in practical
 248 engineering. To verify the accuracy and efficiency of BG, two-dimensional finite
 249 element model is established and harmonic analyses with six rows of hollow steel
 250 trenches are carried out, as shown in Fig. 3. Perfectly matched layers (PML) are added
 251 on the boundaries of soils to prevent the reflection of vibration waves from the bound.
 252 A vertical harmonic load $F_0 = 1000$ N vibrates along the y -direction at the point A away

253 from the left boundary of model to simulate the incident surface waves. l_2 is the distance
254 from the source to the first row of trenches. l_3 is the distance from the last row of
255 trenches to the detection point B for vibration response. The dimensions of the soil
256 substrate are l_4 and l_5 respectively. In this section, the following parameters are
257 considered: $l_1 = 5$ m, $l_2 = 20$ m, $l_3 = 3$ m, $l_4 = 40$ m, $l_5 = 15$ m, the geometrical parameters
258 and material properties of two types of trenches are referred to [Tables 1 and 2](#). The free
259 triangular mesh is adopted for discretizing the model and a mapped mesh is used for
260 the PMLs. The maximum element size is 0.225 m, which is consistent with that of the
261 unit cell models used to calculate the dispersion relations in Section 3.1.

262 To assess the vibration isolation performance of periodic trenches, the transmission
263 attenuation is defined: $TA = 20 \times \log_{10}(u_{y1}/u_{y0})$, the u_{y1} and u_{y0} represent the
264 displacement at the detection point B with and without trenches respectively. The
265 transmission attenuation curves together with the corresponding dispersion curves of
266 two types of periodic hollow steel trenches are shown in [Fig. 4](#), it can be found that the
267 BGs are well coincide with that of attenuation zones (AZs). The interesting feature is
268 that a new AZ2 appears around point A₁ ranging from 18 Hz to 25 Hz in [Fig. 4](#) (a), it
269 is because that Rayleigh waves are forced to transform into hybrid Rayleigh waves
270 traveling at different phase velocity in the frequency region below the resonance (25.4
271 Hz) by the locally resonant trenches and portion of the surface energy leaks into the soil
272 substrate, which results in a surface ground motion attenuation [\[38\]](#). In addition, a new
273 attenuation zone (AZ3) in [Fig. 4](#) (b) exist above the AZ1. It is attributed to that pseudo
274 surface wave modes exist in the area beyond the sound cone (the blue areas), which is

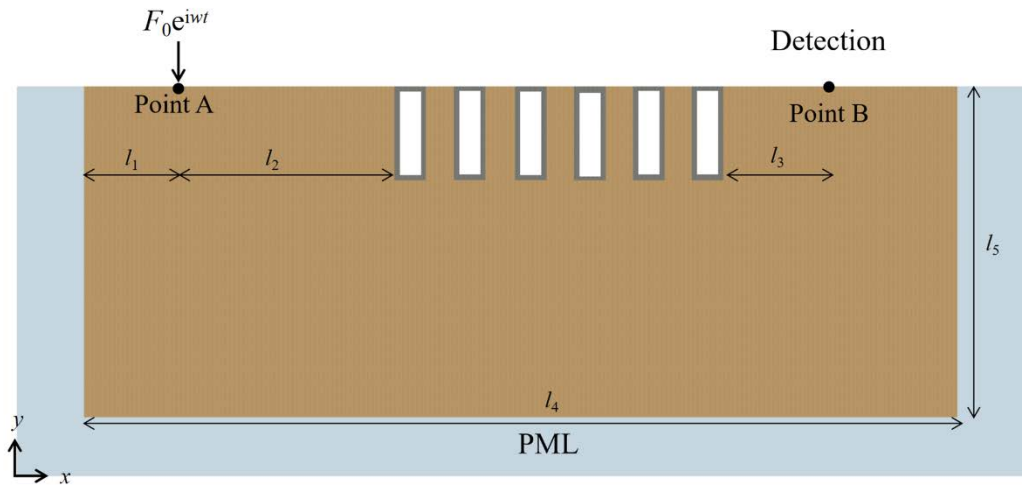
275 contain small bulk-wave components that leak energy into the substrate [17,41]. Further
276 information on pseudo surface waves in periodic structures can be found in references
277 [41-43]. It is interesting to note that the transmission attenuation degree within the
278 Bragg BG is larger than that within the locally resonant BG. As an example, the largest
279 transmission attenuation degree of periodic hollow sealed steel trenches is
280 approximately 23 dB for AZ1 and that for AZ2 is about 12 dB. The largest transmission
281 attenuation degree of periodic hollow unsealed steel trenches is around 31 dB for AZ1,
282 and that for AZ2 is about 12 dB. This occurs due to that the surface wave wavelength
283 at low frequencies is longer than that at high frequencies, resulting in that the number
284 of low-frequency surface waves propagating through the limited amount of unit cells is
285 less than that of high-frequency surface waves. Generally, the transmission attenuation
286 of low-frequency surface waves can be enhanced by growing the number of unit cells
287 to contain more low-frequency surface wavelengths.

288 To further confirm the attenuation of surface waves within BGs, nephograms of
289 displacement field for the system when vibrating at 30 Hz outside the BGs and 55 Hz
290 inside the BG are given in Fig. 5 (a) and (b) respectively. The results indicate that when
291 incident waves at 30 Hz outside the BGs pass through the periodic hollow sealed steel
292 trenches, no obvious attenuation occurs the area behind periodic trenches. However,
293 the incident surface waves at 55 Hz inside the BG are almost totally reflected and
294 concentrated in the soil on the left side of periodic trenches. It is validated that the
295 desired isolation performance can be obtained within BG. Fig. 6 illustrates the
296 attenuation characteristics of the incident surface wave at 55 Hz where the shaded area

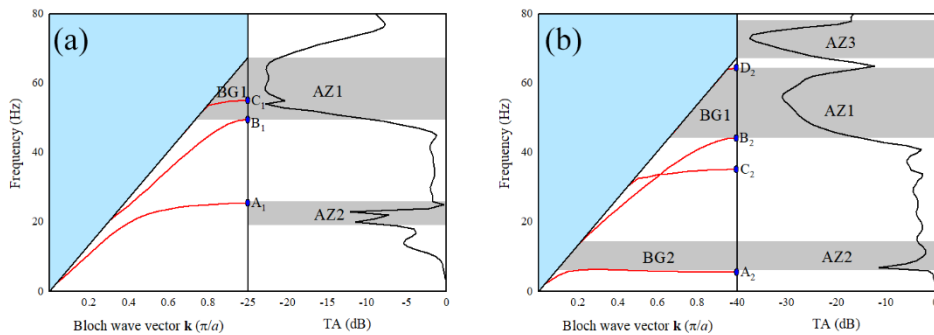
297 represents the location of periodic hollow sealed steel trenches. It is clear that an
298 exponential decay of displacement occurs inside the periodic hollow sealed steel
299 trenches, which is an interference characteristic of Bragg scattering.

300 The comparative study is also conducted to validate the superiority of vibration
301 isolation for two types of proposed periodic hollow steel trenches. Fig. 7 (a) and (b)
302 compares the vibration isolation performance of two types of periodic hollow steel
303 trenches and periodic geofoam-filled trenches by Pu and Shi. The geometrical
304 parameters and material properties of periodic geofoam-filled trenches and is referred
305 to [17]: the width of trench b is 0.3 m, the depth of trench d is 2 m, the lattice constant
306 a is 1 m, the row of trenches is six, the E_{geofoam} is 37 MPa, the ρ_{geofoam} is 60 kg/m³ and
307 ν_{geofoam} is 0.32. The row and geometrical parameters of two types of periodic hollow
308 steel trenches in the comparative study are the same as that of periodic geofoam-filled
309 trenches. Furthermore, the thickness of hollow steel plate c is 0.02 m, and material
310 properties of soils is show in Table 1. The results, as presented in Fig. 7 (a) and (b),
311 indicate that the vibration isolation performances of two types of periodic hollow steel
312 trenches are superior to that of periodic geofoam-filled trenches below 80 Hz. It is
313 because that the impedance of hollow steel trenches is lower than that of geofoam-filled
314 trenches, a smaller impedance means that fewer waves pass through materials [9]. The
315 smaller impedance ratio between the barrier and the adjacent soil is contribute to the
316 vibration reduction more [8,44]. Therefore, the value of TA with two types of periodic
317 hollow steel trenches is bigger than that with periodic geofoam-filled trenches within
318 the BG. Moreover, it is clear that the vibration isolation performance of open trench is

319 better than other wave barriers, since the impedance of air is pretty low compared to
 320 the impedance of soil. Thus, the hollow unsealed steel trench, which is more similar to
 321 the open trench in structure form, can isolate more vibration waves than hollow sealed
 322 steel trench, so the value of TA with periodic hollow unsealed steel trenches is bigger
 323 than that with periodic hollow sealed steel trenches within the BG. Importantly, the use
 324 of periodic hollow steel trenches provides an AZ in the low frequencies below 20 Hz
 325 shown in the first shaded area caused by the local resonance of hollow steel trench. It
 326 means that the proposed periodic hollow steel trenches can be applied to the attenuation
 327 of vibration induced by trains (dominant frequency: 40-60 Hz), and attenuate seismic
 328 waves (dominant frequency: below 20 Hz) as well.

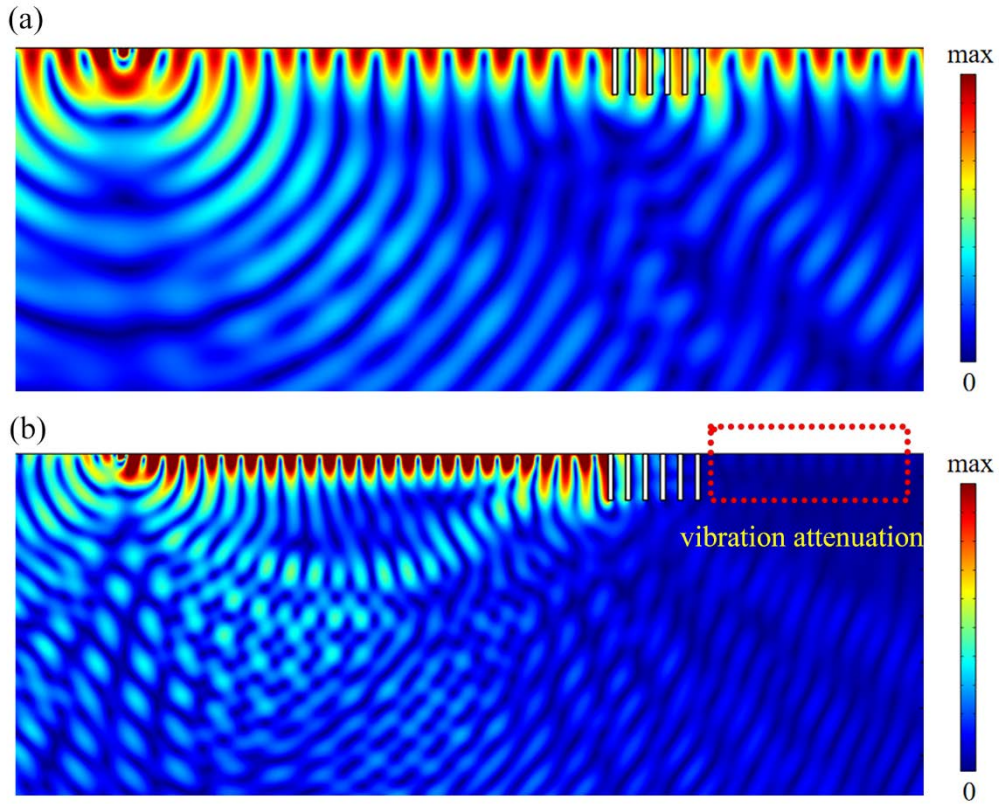


329
330 Fig. 3 Finite element model used for the numerical analysis.

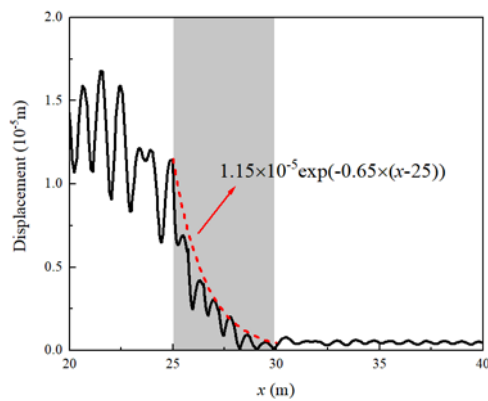


331

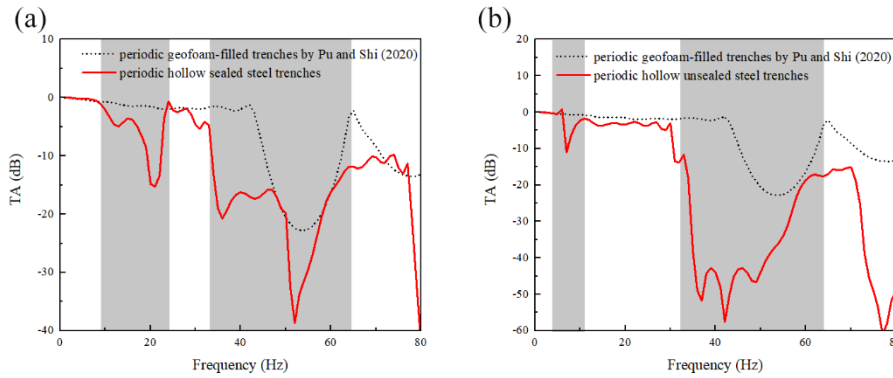
332 Fig. 4 Dispersion relations and transmission attenuation spectra of (a) periodic hollow
 333 sealed steel trenches, (b) periodic hollow unsealed steel trenches.



334
 335 Fig. 5 The nephogram of displacement field for soil-periodic hollow sealed steel
 336 trenches system at frequencies of (a) 30 Hz and (b) 55 Hz.



337
 338 Fig. 6 Attenuation characteristics of the incoming surface waves at 55 Hz. (periodic
 339 hollow sealed steel trenches are situated in the shadow area)



340

341 Fig. 7 Comparison of the vibration isolation effects of periodic in-filled trenches and (a)
 342 periodic hollow sealed steel trenches, (b) periodic hollow unsealed steel trenches.

343

344 3.3 Time domain analysis

345 In this section, the vibration isolation performance of two types of proposed
 346 periodic hollow trenches is analyzed in the time domain. PMLs in Fig. 3 are not suitable
 347 for the time domain analysis, so the low-reflective boundary condition is applied to the
 348 model to avoid the reflection of vibration waves in time domain analysis. The
 349 geometrical parameters and material properties of periodic hollow steel trenches in time
 350 domain analysis are also referred to Table 1 and 2, l_1 , l_2 , l_3 , l_4 , and l_5 are the same as
 351 described in Section 3.2. A 50 Hz (within the BG1 of periodic hollow unsealed steel
 352 trenches) and 7 Hz (within the BG2 of periodic hollow unsealed steel trenches)
 353 harmonic unit displacement load is applied to the point A along the y -direction using
 354 the model in Fig. 3 respectively. Fig. 8 and 9 present the displacement field nephogram
 355 of soils with periodic hollow unsealed steel trenches and without trenches at varying
 356 times as an example to show an explicit attenuation of the wave propagation through
 357 the trenches. The color bar represents the degree of the displacement, red stands for the
 358 maximum displacement. It is worth noting that the incident surface waves (50 Hz)

359 within BG1 (Bragg BG) are almost completely reflected, while the incident surface
360 waves (7 Hz) within BG2 (local resonance BG) are suppressed and confined inside unit
361 cells resulting from the resonance.

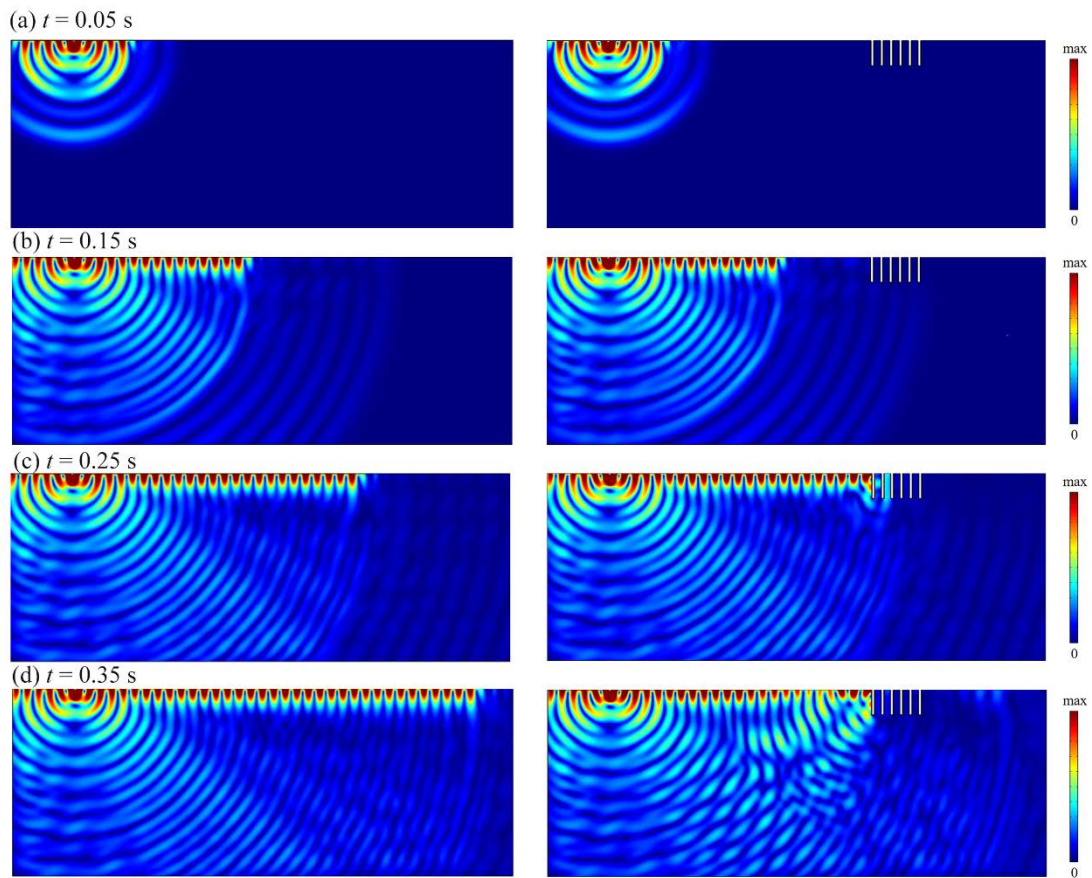
362 In practice, ambient vibration is not harmonic such as vibration induced by trains
363 and seismic vibration, these vibrations are superposed by different frequency vibration.
364 Therefore, this work conducts a field test to obtain practical traffic-induced ground
365 vibrations in Dongguan (Guangdong Province, China) as shown in Fig. 10 (a) and (b),
366 also acquire a practical seismic vibration record from the PEER Ground Database [45]
367 as shown in Fig. 12 (a) and (b). Moreover, the measured acceleration data can be
368 integrated twice to acquire the displacement load, which can be applied at point A along
369 the y-direction in the model for time domain analysis. The type of daily operating
370 elevated intercity train in the field test is CRH6. The INV3062-type vibration signal
371 acquisition instruments and 941B-type ultra-low accelerometers are used. Fig. 10 (c)
372 and (d) show the measured acceleration record and the corresponding Fourier spectrum
373 at 10 m away from the pier in a field are measured when a train runs by approximately
374 100 km/h respectively. It is apparent that the main frequency domain of vibrations
375 induced by this train is around 40-60 Hz. The acceleration data are integrated twice to
376 acquire the displacement load to add to the point A along the y-direction. The rows,
377 materials and geometric parameters of periodic hollow sealed steel trenches are the
378 same as above. Fig. 11 (a) shows vertical acceleration responses at the detection point
379 B with two kinds of periodic hollow steel trenches and without trenches subjected to
380 railway excitation. It can be spotted that the accelerations behind the periodic hollow

381 steel trenches are significantly reduced. Fig. 11 (b) presents the corresponding Fourier
382 spectrum of acceleration responses and it can be found that the vibration induced by
383 trains is dramatically reduced within the BGs. The acceleration amplitudes with
384 periodic hollow sealed steel trenches and with periodic hollow unsealed steel trenches
385 are reduced by 51% and 71% respectively, when comparing with that without trenches.

386 Data with respect to diverse earthquakes show that the dominant frequencies of
387 seismic waves span the range of 1–20 Hz [31,46]. Fig. 12 (a) and (b) present the 2008
388 Iwate (Japan) AKT019UD records and the Fourier spectrum acquired from the PEER
389 Ground Database [45]. It can be seen that the dominant frequencies of Iwate seismic
390 waves are below 20 Hz. To verify the shielding capability of periodic hollow steel
391 trenches for seismic vibration, the displacement load of Iwate AKT019UD records
392 added on the point A along the y-direction. The rows, materials and geometric
393 parameters of periodic hollow sealed steel trenches remain the same as above. Fig. 13
394 shows the acceleration responses and corresponding Fourier spectra under the
395 excitation of Iwate (Japan) AKT019UD record with periodic hollow steel trenches and
396 without trenches. The acceleration amplitudes with periodic hollow sealed steel
397 trenches and with periodic hollow unsealed steel trenches are reduced by 32% and 31%
398 respectively.

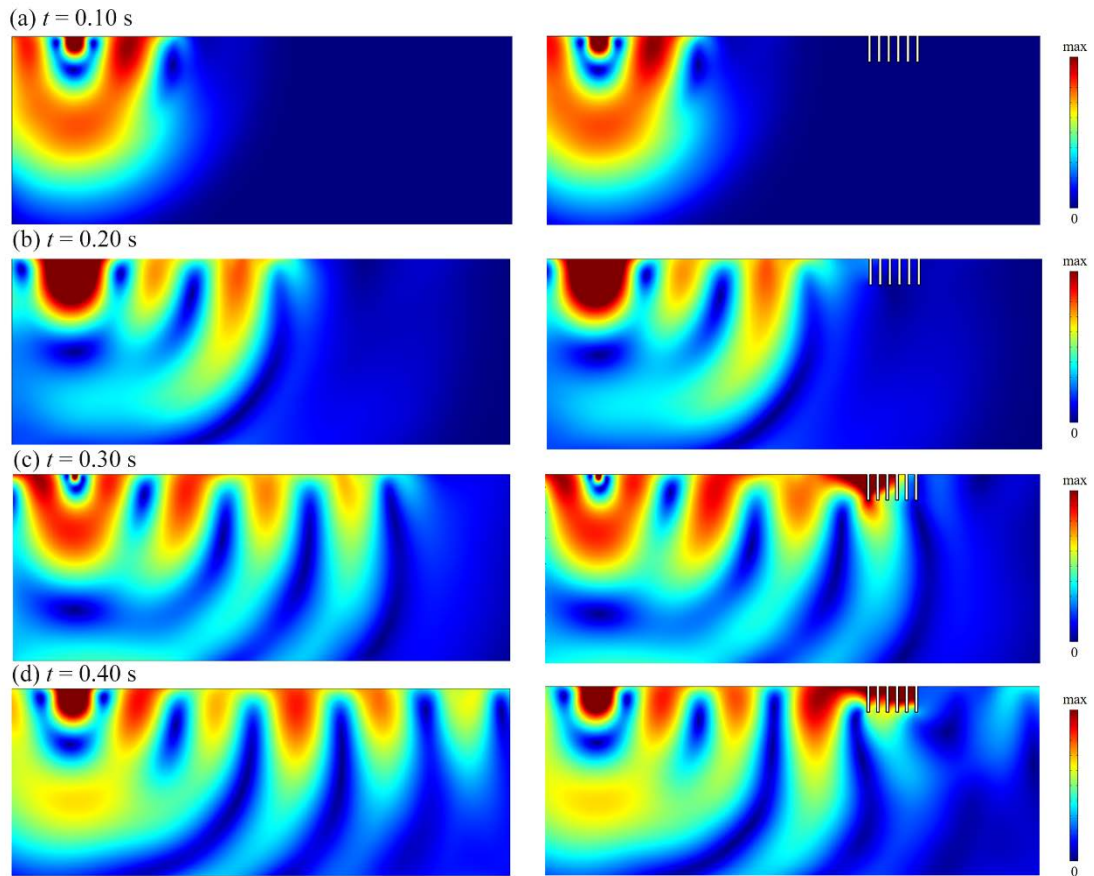
399 The time domain analysis indicates that the use of proposed periodic hollow steel
400 trenches could effectively isolate the vibration induced by trains (dominant frequency:
401 40-60 Hz) and seismic waves (dominant frequency: below 20 Hz), as hollow steel
402 trenches exhibit Bragg and local resonance BG in the middle and low frequency range

403 respectively. [Table 5](#) summarizes the vibration isolation results for the periodic hollow
404 steel trenches in frequency and time domain analysis.



405

406 Fig. 8 Transient displacement field nephogram for soils with periodic hollow unsealed
407 steel trenches and without trenches at frequencies of 50 Hz when (a) $t = 0.05$ s, (b) $t =$
408 0.15 s, (c) $t = 0.25$ s and (d) $t = 0.35$ s.

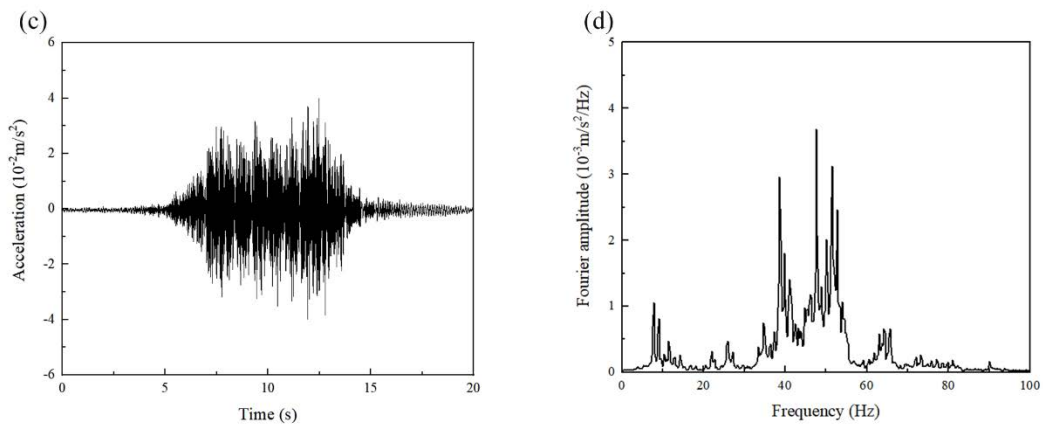


409

410 Fig. 9 Transient displacement field nephogram for soils with periodic hollow unsealed

411 steel trenches and without trenches at frequencies of 7 Hz when (a) $t = 0.10$ s, (b) $t =$

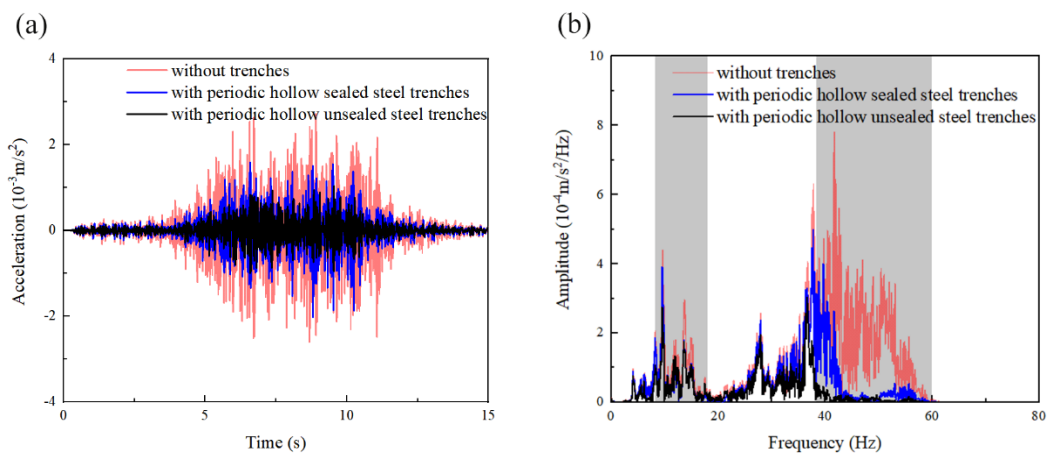
412 0.20 s, (c) $t = 0.30$ s and (d) $t = 0.40$ s.



413

414 Fig. 10 Vibration response in the field induced by the intercity railway: (a) (b) field

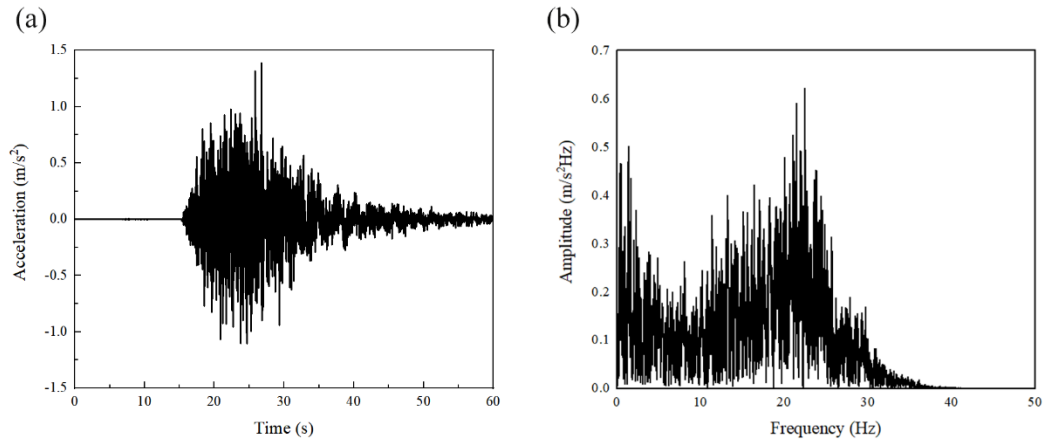
415 measure; (c) vertical acceleration record; (d) Fourier spectrum.



416

417 Fig. 11 (a) Vertical acceleration responses at the detection point B and (b) corresponding

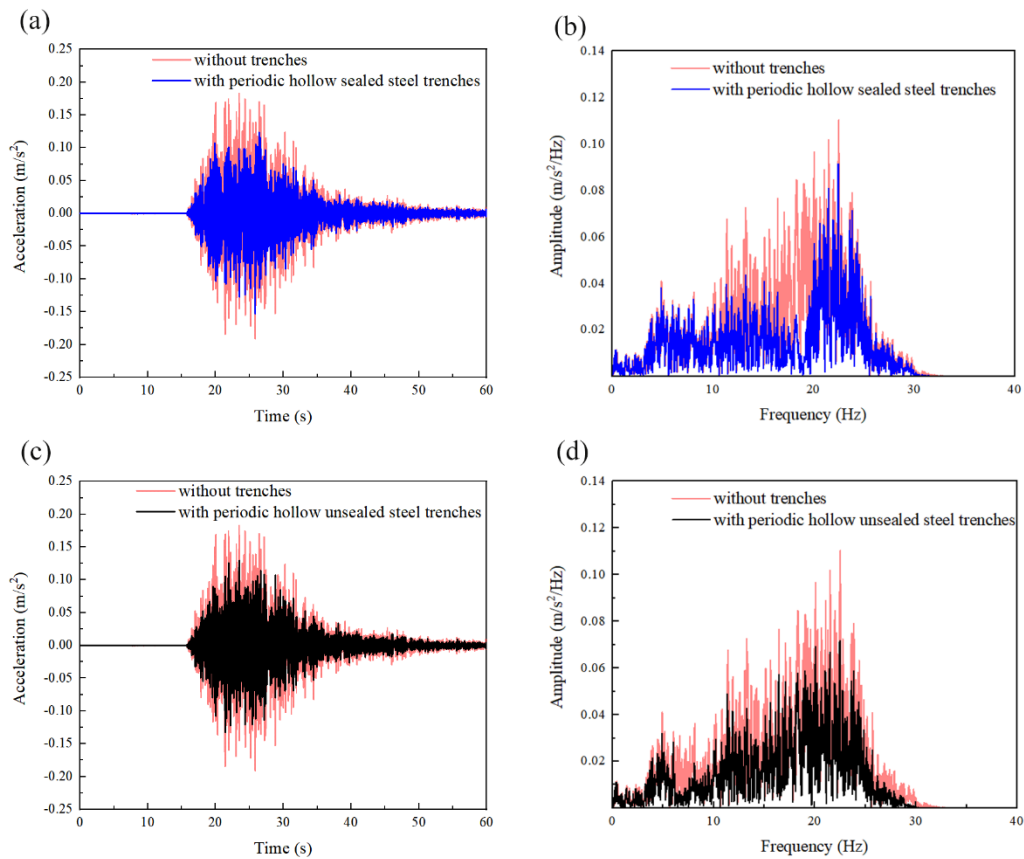
418 Fourier spectra with and without trenches.



419

420

Fig. 12 (a) Iwate (Japan) AKT019UD record; (b) Fourier spectrum.



421

422 Fig. 13 Vertical acceleration responses under the excitation of Iwate (Japan)

423 AKT019UD record with and corresponding Fourier spectra: (a-b) with periodic hollow

424 sealed steel trenches and without trenches, (c-d) with periodic hollow unsealed steel

425 trenches and without trenches.

426 Table 5. Summary of vibration isolation results for the periodic hollow steel trenches.

427 (geometrical parameters and material properties are referred to Table 1 and 2)

Types of wave barriers	Frequency domain (largest TA degree)		Time domain (reduction of acceleration amplitudes)	
	AZ1	AZ2	seismic load	train load
Periodic hollow sealed steel trenches	12 dB	23 dB	32%	51%
Periodic hollow unsealed steel trenches	12 dB	31 dB	31%	71%

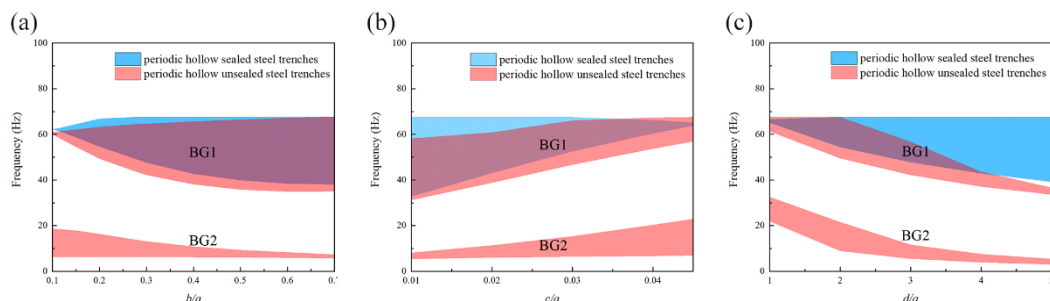
428

429 3.4 Effect of geometric parameters

430 The frequency domain and time domain analysis above demonstrate that the
431 proposed periodic hollow steel trenches can be appropriate for the application in
432 isolating vibration induced by trains and attenuating seismic waves. To further illustrate
433 the mechanism of BG and explore the optimization of structure design, the influence of
434 geometrical parameters on the BGs of hollow steel trench are discussed in this section.
435 The variation of the bound frequency of two types of periodic hollow steel trenches
436 with the change of a single geometrical parameter is analyzed in Fig. 14. The other
437 materials and geometric parameters of periodic hollow sealed steel trenches are referred
438 to Table 1 and 2. When a single parameter is changed, the other parameters remain
439 unaltered.

440 Fig 14 (a) shows the effect of the ratio b/a on the BGs. As the increase of b/a , the
441 upper and lower bound of BG1 for two types of periodic hollow steel trenches are
442 moved to higher and lower frequencies respectively, so the width of BG1 increases with
443 the b/a increases. However, the upper boundary decreases of periodic hollow unsealed
444 steel trenches as the b/a increases, the width of BG2 decreases. Additionally, though
445 the transmission attenuation spectrums in Fig. 4 (a) demonstrates that periodic hollow

446 sealed steel trenches can be used to attenuate vibration at lower frequencies (18-25 Hz)
 447 as shown in AZ2, there is no BG2 for periodic hollow sealed steel trenches at lower
 448 frequency in the dispersion curves in Fig. 2 (a). Therefore, we do not discuss the effect
 449 of materials and geometric parameters on lower frequency BGs of periodic hollow
 450 sealed steel trenches. Fig 14 (b) presents the effect of the ratio c/a on the BGs, it is
 451 observed that the increase of c/a leads to the shifting toward the higher frequency bound
 452 of BG1 for periodic hollow steel trenches and narrowing of the BG width. However,
 453 the BG2 widens with the increase of c/a , because the upper frequency bound of BG2
 454 increases when the lower bound frequency is basically unchanged. It means that the
 455 increase of thickness of steel plate c is more significant for isolating lower frequency
 456 waves such as seismic waves in practical engineering. In Fig 14 (c), the upper frequency
 457 bound of periodic hollow unsealed steel trenches decreases when d/a is greater than 2,
 458 the BG1 width of that also reduces with the increase of d/a . Whereas, the BG1 of
 459 periodic hollow sealed steel trenches widens with the rise of d/a . In addition, the BG2
 460 of periodic hollow unsealed steel trenches shift the lower frequency bound but the width
 461 tends to narrow with the increase of d/a .



462

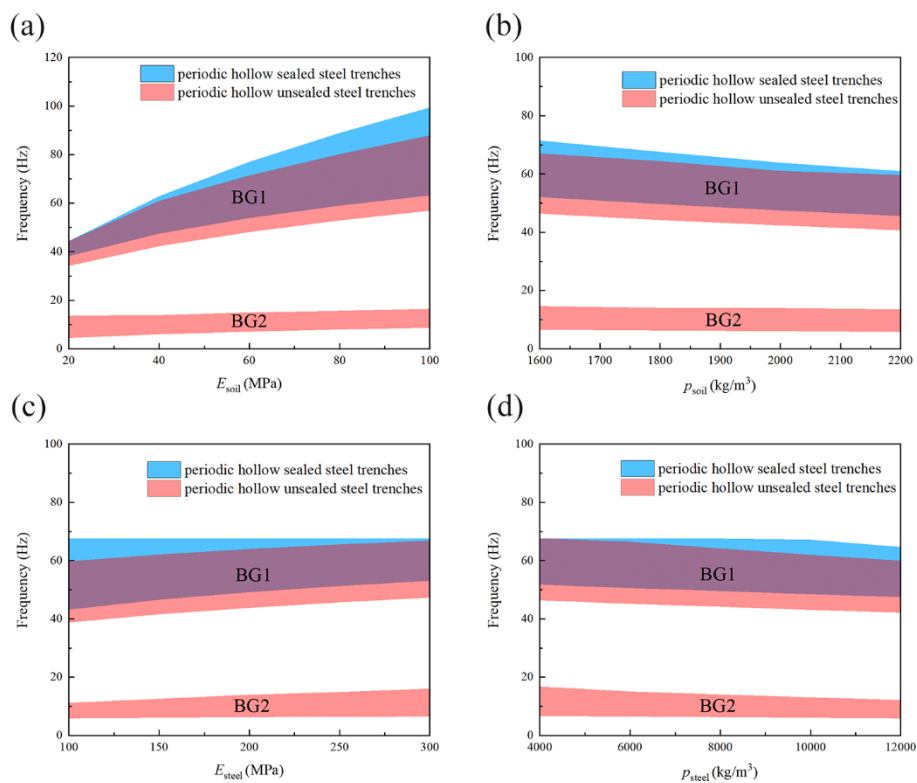
463 Fig. 14 Effect of different geometric parameters for two types of periodic hollow steel
464 trenches on the BGs: (a) ratio of the width b to the lattice constant a ; (b) ratio of the
465 thickness c to the lattice constant a ; (c) ratio of the depth d to the lattice constant a .

466 *3.5 Effect of material parameters*

467 The relation between geometric parameters and BGs are analyzed in the previous
468 section and it is available for modifying the geometric parameters to tune the properties
469 of the BG, especially its location and width. In this section, the effect of material
470 parameters of soils and steel on the BGs are discussed as shown in Fig. 15.

471 Fig. 15 (a) and (b) presents the variation of the bound frequency of two types of
472 periodic hollow steel trenches with the change of Young's modulus and mass density
473 of soil respectively. When the Young's modulus of soil increases from 20 MPa to 100
474 MPa, the upper and lower frequencies of BG1 for two types of periodic hollow steel
475 trenches rise dramatically, while the BG1 width enlarges significantly. Although the
476 BG2 width of periodic hollow unsealed steel trenches remain basically constant with
477 the increase of Young's modulus of soil, its location is moved to the higher frequencies
478 gradually. From Fig. 15 (b), as the mass density of soil increases from 1600 kg/m³ to
479 2200 kg/m³, the upper and lower bound frequencies of BG1 for two types of periodic
480 hollow steel trenches decrease substantially and the bound frequency of BG2 for
481 periodic hollow unsealed steel trenches keep almost unchanged. Fig. 15 (c) and (d)
482 present effects of the Young's modulus and mass density of steel on BG2 for two types
483 of periodic hollow steel trenches. The rise of Young's modulus of steel causes the
484 increase of upper and lower bound frequencies of BG1 for periodic hollow unsealed

485 steel trenches in Fig. 15 (c), and it can contribute to the enlarging of BG2 width, which
 486 means that increasing Young's modulus of steel is a desired method to widen the width
 487 of low frequency BG to attenuate vibration such as seismic waves. As can be seen from
 488 Fig. 15 (d), BG1s descend gradually and steadily are shifted toward the lower frequency
 489 as the increase of mass density of steel. Though the lower bound of BG2 for periodic
 490 hollow unsealed steel trenches keeps basically unchanged, the BG2 width is turned to
 491 be narrower because the upper bound frequency moves toward lower frequencies.



492
 493 Fig. 15 Effect of soil and steel material parameters: (a) the Young's modulus of soil; (b)
 494 the mass density of soil; (c) the Young's modulus of steel; (d) the mass density of steel.

495 4. Conclusion

496 In summary, two novel types of periodic hollow steel trenches with Bragg band gap
 497 and locally resonant BG are proposed. Based on Bloch theory and finite element

498 method, the dispersion relations are calculated and the generation mechanism of BGs
499 are clarified. The effectiveness of the periodic hollow steel trenches on the surface
500 waves attenuation is confirmed by both frequency domain and time domain analysis.
501 Furthermore, the effects of several significant geometric parameters (the width and
502 depth of trenches, the thickness of steel plates) and several materials parameters
503 (Young's modulus and mass density of soils and steel) on the the BGs have been
504 analyzed respectively. The conclusions drawn are as follows:

505 (1) The proposed periodic hollow steel trenches feature both a Bragg BG and a local
506 resonance BG simultaneously. The Bragg BG around middle frequencies is
507 induced stemming from system's periodicity, which is of interest for control
508 ambient vibration such as vibrations induced by trains. The local resonance BG
509 appears below 20 Hz due to occurrence of unit cell local resonance, which can
510 contribute to the isolation of seismic vibration.

511 (2) When the frequencies of incident surface waves fall into the local resonance BG,
512 wave energy is confined and suppressed inside the unit cell structures. If the
513 frequencies of incident surface waves are within the Bragg BG, incident surface
514 waves can be almost fully reflected and an exponential decay of the
515 transmission occurs inside the periodic hollow sealed steel trenches.

516 (3) The Bragg BG width of two types of periodic hollow steel trenches increases
517 with an increase of trench width or decrease of steel plate thickness, while the
518 local resonance BG width decreases with such the variation of parameters. The
519 rise of depth of trenches results in the decline of both Bragg BG and local

520 resonance BG width of periodic hollow unsealed steel trenches, but causes the
521 increase of Bragg BG of periodic hollow sealed steel trenches.

522

523 **Acknowledgements**

524 The work described in this paper was fully supported by grants from the National
525 Natural Science Foundation of China (Grant Nos. 51908554, 52008033 and U1934209)
526 and Hunan Provincial Natural Science Foundation of China (Project No. 2020JJ5712).

527

528 **References**

529 [1] Comina C, Foti S. Surface wave tests for vibration mitigation studies. *J Geotech*
530 *Geoenviron Eng* 2007;133:1320–4.

531 [2] Toygar O, Ulgen D. A full-scale field study on mitigation of environmental ground
532 vibrations by using open trenches. *Build Environ* 2021;203:108070.

533 [3] Lu J, Xu B, Wang J. Numerical analysis of isolation of the vibration due to moving
534 loads using pile rows. *J Sound Vib* 2009;319:940–62.

535 [4] Lyratzakis A, Tsompanakis Y, Psarropoulos PN. Efficient mitigation of high-speed
536 train vibrations on adjacent reinforced concrete buildings. *Constr Build Mater*
537 2022;314:125653.

538 [5] Saikia A. Numerical study on screening of surface waves using a pair of softer
539 backfilled trenches. *Soil Dyn Earthq Eng* 2014;65:206–13.

540 [6] Celebi E, Firat S, Beyhan G, Cankaya I, Vural I, Kirtel O. Field experiments on
541 wave propagation and vibration isolation by using wave barriers. *Soil Dyn Earthq*

- 542 Eng 2009;29:824–33.
- 543 [7] Alzawi A, Naggar MH. Full scale experimental study on vibration scattering using
544 open and in-filled (Geofoam) wave barriers. *Soil Dyn Earthq Eng* 2011;31:306–17.
- 545 [8] Ulgen D, Toygar O. Screening effectiveness of open and in-filled wave barriers: a
546 full-scale experimental study. *Constr Build Mater* 2015;86:12–20.
- 547 [9] Majumder M, Ghosh P, Rajesh S. An innovative vibration barrier by intermittent
548 geofoam-a numerical study. *Geomech Eng* 2017;13(2):269–84.
- 549 [10] Rizvi SMF, Wang K, Jalal FE, Tu Y. Evaluation of open and filled (TDA and RSM)
550 trenches efficacy on vibration screening caused by transient loads. *Transp Geotech*
551 2022;35:100770.
- 552 [11] Kushwaha MS, Halevi P, Dobrzynski L, Djafari-Rouhani B. Acoustic band
553 structure of periodic elastic composites. *Phys Rev Lett* 1993;71(13):2022–25.
- 554 [12] Kushwaha MS, Halevi P, Martínez G, Dobrzynski L, Djafari-Rouhani B. Theory
555 of acoustic band structure of periodic elastic composites. *Phys Rev B*
556 1994;49:2313–22.
- 557 [13] Vasseur JO, Deymier PA, Chenni B, Djafari-Rouhani B, Dobrzynski L, Prevost D.
558 Experimental and theoretical evidence for the existence of absolute acoustic band
559 gaps in two-dimensional solid phononic crystals. *Phys Rev Lett*. 2001;86(14):
560 3012–15.
- 561 [14] Liu Z, Zhang X, Mao Y, Zhu YY, Yang Z, Chan CT, Sheng P. Locally resonant
562 sonic materials. *Science* 2000;289(5485):1734–36.
- 563 [15] Li Z, Hu H, Wang X. A new two-dimensional elastic metamaterial system with

- 564 multiple local resonances. *Int J Mech Sci* 2018;149:273–84.
- 565 [16] Jiang W, Yin M, Liao Q, Xie L, Yin G. Three-dimensional single-phase elastic
566 metamaterial for low-frequency and broadband vibration mitigation. *Int J Mech*
567 *Sci* 2021;190:106023.
- 568 [17] Pu X, Shi Z. Broadband surface wave attenuation in periodic trench barriers. *J*
569 *Sound Vib* 2020;468:115130.
- 570 [18] Pu X, Meng Q, Shi Z. Experimental studies on surface-wave isolation by periodic
571 wave barriers. *Soil Dyn Earthq Eng* 2020;130:106000.
- 572 [19] Cai C, Gao L, He X, Zou Y, Yu K, Wu D. The surface wave attenuation zone of
573 periodic composite in-filled trenches and its isolation performance in train-
574 induced ground vibration isolation. *Comput Geotech* 2021;139:104421.
- 575 [20] Huang J, Liu W, Shi Z. Surface-wave attenuation zone of layered periodic
576 structures and feasible application in ground vibration reduction. *Constr Build*
577 *Mater* 2017;141:1–11.
- 578 [21] Meng L, Cheng Z, Shi Z. Vibration mitigation in saturated soil by periodic in-filled
579 pipe pile barriers. *Comput Geotech* 2020;124:103633.
- 580 [22] Jiang Y, Meng F, Chen Y, Zheng Y, Chen X, Zhang J, Huang X. Vibration
581 attenuation analysis of periodic underground barriers using complex band
582 diagrams. *Comput Geotech* 2020;128:103821.
- 583 [23] Huang J, Shi Z. Vibration Reduction of Plane Waves Using Periodic In-Filled Pile
584 Barriers. *J Geotech Geoenviron Eng* 2015;141:04015018.
- 585 [24] Lei L, Miao L, Li C, Liang X, Wang J. Locally resonant periodic wave barriers for

586 vibration isolation in subway engineering. *KSCE J Civ Eng.* 2021;25(4):1239–51.

587 [25] Du Q, Zeng Y, Xu Y, Yang H, Zeng Z. H-fractal seismic metamaterial with
588 broadband low-frequency bandgaps. *J Phys D Appl Phys* 2018;51:105104.

589 [26] Muhammad, Lim CW, Reddy JN. Built-up structural steel sections as seismic
590 metamaterials for surface wave attenuation with low frequency wide bandgap in
591 layered soil medium. *Eng Struct* 2019;188:440–51.

592 [27] Zeng Y, Xu Y, Yang H, Muzamil M, Xu R, Deng K, Peng P, Du Q. A Matryoshka-
593 like seismic metamaterial with wide band-gap characteristics. *Int J Solids Struct*
594 2020;185-186:334–41.

595 [28] Wang X, Wan S, Nian Y, Zhou P, Zhu Y. Periodic in-filled pipes embedded in semi-
596 infinite space as seismic metamaterials for filtering ultra-low-frequency surface
597 waves. *Constr Build Mater* 2021;313:125498.

598 [29] Huang T, Ren X, Zeng Y, Zhang Y, Luo C, Zhang X, Xie Y. Based on auxetic foam:
599 A novel type of seismic metamaterial for Lamb waves. *Eng Struct*
600 2021;246:112976.

601 [30] Wu X, Wen Z, Jin Y, Rabczuk t, Zhuang X, Djafari-Rouhani B. Broadband
602 Rayleigh wave attenuation by gradient metamaterials. *Int J Mech Sci*
603 2021;205:106592.

604 [31] Miniaci M, Krushynska A, Bosia F, Pugno NM. Large scale mechanical
605 metamaterials as seismic shields. *New J Phys* 2016;18:083041.

606 [32] Pennec Y, Djafari-Rouhani B, Larabi H, Vasseur JO, Hladky-Hennion AC. Low-
607 frequency gaps in a phononic crystal constituted of cylindrical dots deposited on

608 a thin homogeneous plate. *Phys Rev B* 2008;78:104105.

609 [33] Wu TT, Huang Z, Tsai TC, Wu TC. Evidence of complete band gap and resonances
610 in a plate with periodic stubbed surface. *Appl Phys Lett* 2008;93:111902.

611 [34] Achaoui Y, Khelif A, Benchabane S, Robert L, Laude V. Experimental observation
612 of locally-resonant and Bragg band gaps for surface guided waves in a phononic
613 crystal of pillars. *Phys Rev B* 2011;83:104201.

614 [35] Jin Y, Pennec Y, Bonello B, Honarvar H, Dobrzynski L, Djafari-Rouhani B,
615 Hussein MI. Physics of surface vibrational resonances: pillared phononic crystals,
616 metamaterials, and metasurfaces. *Rep Prog Phys* 2021;84:086502.

617 [36] Jin Y, Fernez N, Pennec Y, Bonello B, Moiseyenko RP, H'emon S, Pan Y, Djafari-
618 Rouhani B. Tunable waveguide and cavity in a phononic crystal plate by
619 controlling whispering-gallery modes in hollow pillars. *Phys Rev B* 2016;93:
620 054109.

621 [37] Jin Y, Pennec Y, Pan Y, Djafari-Rouhani B. Phononic crystal plate with hollow
622 pillars connected by thin bars. *J Phys D Appl Phys* 2017;50:035301.

623 [38] Palermo A, Vitali M, Marzani A. Metabarriers with multi-mass locally resonating
624 units for broad band Rayleigh waves attenuation. *Soil Dyn Earthq Eng*
625 2018;113:265–77.

626 [39] Assouar MB, Oudich M. Dispersion curves of surface acoustic waves in a two-
627 dimensional phononic crystal. *Appl Phys Lett* 2011;99(12):123505.

- 628 [40] Achaoui Y, Khelif A, Benchabane S, Robert L, Laude V. Experimental observation
629 of locally-resonant and Bragg band gaps for surface guided waves in a phononic
630 crystal of pillars. Phys Rev B 2011;83(10):104201.
- 631 [41] Graczykowski B, Alzina F, Gomis-Bresco J, Torres CMS. Finite element analysis
632 of true and pseudo surface acoustic waves in one dimensional phononic crystals. J
633 Appl Phys 2016;119:025308.
- 634 [42] Veres IA, Berer T. Complexity of band structures: semi-analytical finite element
635 analysis of one-dimensional surface phononic crystals. Phys Rev B 2012;86:104304.
- 636 [43] Glass NW, Maradudin AA. Leaky surface-elastic waves on both flat and strongly
637 corrugated surfaces for isotropic, nondissipative media. J Appl Phys 1983;54:796–
638 805.
- 639 [44] Massarsch K. Vibration isolation using gas-filled cushions. In: Proceedings of the
640 Geo-Frontiers 2005 congress. American Society of Civil Engineers, Austin, Texas;
641 2005.
- 642 [45] PEER. Peer Ground Motion Database; 2012. <http://peer.berkeley.edu/peer>
643 [ground_motion_database](http://peer.berkeley.edu/peer).
- 644 [46] Gadallah MR, Fisher RL. Applied Seismology: A comprehensive Guide to Seismic
645 Theory and Application (PennWell Books, 2005).
- 646
- 647